



HAL
open science

Rotational spectrum of methoxyamine up to 480 GHz: a laboratory study and astronomical search

L. Kolesnikova, B. Tercero, E. R. Alonso, J. -C. Guillemin, J. Cernicharo, J. L. Alonso

► To cite this version:

L. Kolesnikova, B. Tercero, E. R. Alonso, J. -C. Guillemin, J. Cernicharo, et al.. Rotational spectrum of methoxyamine up to 480 GHz: a laboratory study and astronomical search. *Astronomy and Astrophysics - A&A*, 2018, 609, pp.A24. 10.1051/0004-6361/201730744 . hal-01685697

HAL Id: hal-01685697

<https://univ-rennes.hal.science/hal-01685697>

Submitted on 27 Apr 2018

HAL is a multi-disciplinary open access archive for the deposit and dissemination of scientific research documents, whether they are published or not. The documents may come from teaching and research institutions in France or abroad, or from public or private research centers.

L'archive ouverte pluridisciplinaire **HAL**, est destinée au dépôt et à la diffusion de documents scientifiques de niveau recherche, publiés ou non, émanant des établissements d'enseignement et de recherche français ou étrangers, des laboratoires publics ou privés.

Rotational spectrum of methoxyamine up to 480 GHz: a laboratory study and astronomical search[★]

L. Kolesniková¹, B. Tercero², E. R. Alonso¹, J.-C. Guillemin³, J. Cernicharo², and J. L. Alonso¹

¹ Grupo de Espectroscopia Molecular (GEM), Edificio Quifima, Área de Química-Física, Laboratorios de Espectroscopia y Bioespectroscopia, Parque Científico UVa, Unidad Asociada CSIC, Universidad de Valladolid, 47011 Valladolid, Spain
e-mail: lucie.kolesnikova@uva.es

² Instituto de Ciencia de Materiales de Madrid, CSIC, C/ Sor Juana Inés de la Cruz 3, 28049 Cantoblanco, Spain

³ Institut des Sciences Chimiques de Rennes, École Nationale Supérieure de Chimie de Rennes, CNRS, UMR 6226, 11 Allée de Beaulieu, CS 50837, 35708 Rennes Cedex 7, France

Received 7 March 2017 / Accepted 26 September 2017

ABSTRACT

Aims. Methoxyamine is a potential interstellar amine that has been predicted by gas-grain chemical models for the formation of complex molecules. The aim of this work is to provide direct experimental frequencies of its ground-vibrational state in the millimeter- and submillimeter-wave regions to achieve its detection in the interstellar medium.

Methods. Methoxyamine was chemically liberated from its hydrochloride salt, and its rotational spectrum was recorded at room temperature from 75 to 480 GHz using the millimeter-wave spectrometer in Valladolid. Many observed transitions revealed *A–E* splitting caused by the internal rotation of the methyl group, which had to be treated with specific internal rotation codes.

Results. Over 400 lines were newly assigned for the most stable conformer of methoxyamine, and a precise set of spectroscopic constants was obtained. Spectral features of methoxyamine were then searched for in the Orion KL, Sgr B2, B1-b, and TMC-1 molecular clouds. Upper limits to the column density of methoxyamine were derived.

Key words. astrochemistry – ISM: molecules – line: identification – astronomical databases: miscellaneous

1. Introduction

Molecular line surveys of massive star-forming regions such as the Orion KL hot core or the Galactic-center hot cores Sgr B2(N) and (M) have shown very complex chemistry through the detection of a large variety of molecules (Cernicharo et al. 2016; Belloche et al. 2013). Of these molecules, amines have received particular attention because they participate in the synthesis of amino acids, the basic units of proteins. Although the original interstellar detection of glycine (Kuan et al. 2003), the simplest amino acid, has been called into doubt (Snyder et al. 2005; Jones et al. 2007; Cunningham et al. 2007), the discovery of glycine in dust samples from comet Wild 2 (Elsila et al. 2009) and in the coma of 67P/Churyumov-Gerasimenko (Altwegg et al. 2016) shows that these types of biomolecules can be formed under cosmic conditions. In addition, several laboratory experiments of the interstellar icy grains analogs have demonstrated that formation of diverse amines and amino acids in the interstellar medium (ISM) is possible (Bernstein et al. 2002; Caro et al. 2002; Zheng & Kaiser 2010; Kim & Kaiser 2011). Spectroscopic characterization and subsequent search for chemically similar species or their possible precursors thus create an important target for astrochemistry.

To the best of our knowledge, only a few molecules containing the $-\text{NH}_2$ group have been confidently detected in the ISM: formamide (NH_2CHO ; Rubin et al. 1971), methylamine

(CH_3NH_2 ; Kaifu et al. 1974; Fourikis et al. 1974), cyanamide (NH_2CN ; Turner et al. 1975), acetamide (CH_3CONH_2 ; Hollis et al. 2006), and aminoacetonitrile ($\text{NH}_2\text{CH}_2\text{CN}$; Belloche et al. 2008). Urea ($(\text{NH}_2)_2\text{CO}$), a molecule with two $-\text{NH}_2$ groups, has been detected only tentatively (Remijan et al. 2014). Of these detected molecules, only two belong to the category of amines; nevertheless, the gas-grain chemical model for the formation of complex molecules predicts that more interstellar amines, such as methoxyamine (CH_3ONH_2), hydroxylamine (NH_2OH) or hydroxymethylamine (HOCH_2NH_2), can be generated with significant abundances (Garrod et al. 2008). The interstellar formation of methoxyamine is proposed through a direct reaction between CH_3O and NH_2 radicals on the grains at temperatures around 50 K (Garrod et al. 2008). It is predicted to remain on the grains until the temperature of ~ 100 K is reached, when it starts to desorb into the gas phase. The peak gas-phase abundance of methoxyamine in the star-forming regions is then predicted at the approximate temperature of 120 K (Garrod et al. 2008).

While hydroxylamine has been actively searched for toward several interstellar sources (Pulliam et al. 2012; McGuire et al. 2015), no such trials have been conducted for methoxyamine, probably because we have only insufficient laboratory information. The most stable conformation of methoxyamine has the $-\text{NH}_2$ group in the *trans*-position with respect to the $-\text{CH}_3$ group (see Fig. 1) and was studied in the gas phase from 8 to 39.5 GHz by Stark-modulation spectroscopy (Fong et al. 1974). Since the rotational constants were obtained from the least-squares fit of four hyperfine-free *a*-type *R*-branch transitions with J'' and

[★] Table 3 is only available at the CDS via anonymous ftp to cdsarc.u-strasbg.fr (130.79.128.5) or via <http://cdsarc.u-strasbg.fr/viz-bin/qcat?J/A+A/609/A24>

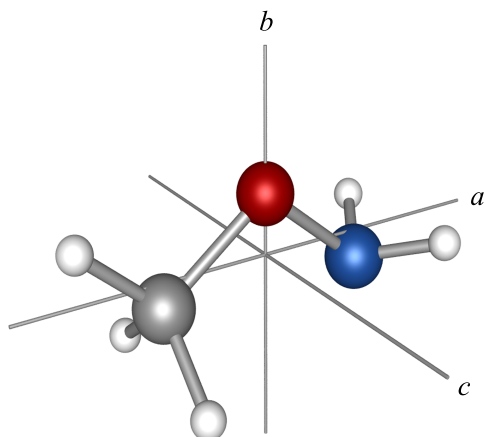


Fig. 1. Equilibrium C_s symmetry structure of the most stable form of methoxyamine.

$K_a'' \leq 1$, they do not provide accurate predictions for the rotational spectrum at higher J and K_a values. At the 67% confidence level, uncertainties of up to 3, 8, and 13 MHz can be estimated for a -type R -branch transitions with $J'' = 6, 12,$ and 18 , respectively. These transitions at the temperature of 120 K fall exactly into the range of millimeter-wave surveys that are provided by several astrophysical instruments, as shown in Fig. 2, and with these uncertainties, it is not possible to confidently search for methoxyamine. Lack of the accurate laboratory millimeter-wave data thus prompted new spectroscopic studies of methoxyamine over the frequency range from 75 to 480 GHz. More than 400 spectral features were newly assigned, which significantly extended the range of J and K_a quantum numbers, and the features were used to search for methoxyamine in Orion KL and Sgr B2 molecular clouds.

2. Experimental details

Methoxyamine is a colorless liquid with a boiling point at 48.1 °C (Bissot et al. 1957), and it was synthesized by reaction of liquid 1,8-diazabicyclo[5.4.0]undec-7-ene injected in excess (1.5 equivalent) through a septum in a two-necked flask containing solid methoxyamine hydrochloride and fitted on a vacuum line. The reaction product was collected in a U-tube trap cooled by liquid nitrogen and was used without any further purification. Methoxyamine was thus obtained in a 70% yield.

The room-temperature rotational spectrum was measured from 75 to 480 GHz using the millimeter-wave spectrometer at the University of Valladolid, which generates the millimeter-wave radiation by multiplying the fundamental synthesizer frequency (≤ 20 GHz) by amplifier-multiplier chains (multiplication factors of 6, 9, 12, 18, and 24 in this case). A detailed description of the experimental setup has been given elsewhere (Daly et al. 2014). The synthesizer output was frequency modulated at a modulation frequency of 10.2 kHz and a modulation depth of between 10 and 30 kHz. After passing the radiation through the free-space cell (see the single- and double-pass configurations in Daly et al. 2014), the signal was detected by zero-bias detectors and was demodulated by a lock-in amplifier tuned to twice the modulation frequency. This demodulation process gives rise to a shape of the lines that approximates the second derivative of a Gaussian function. The experimental uncertainty of the isolated symmetric lines is estimated to be better than 50 kHz.

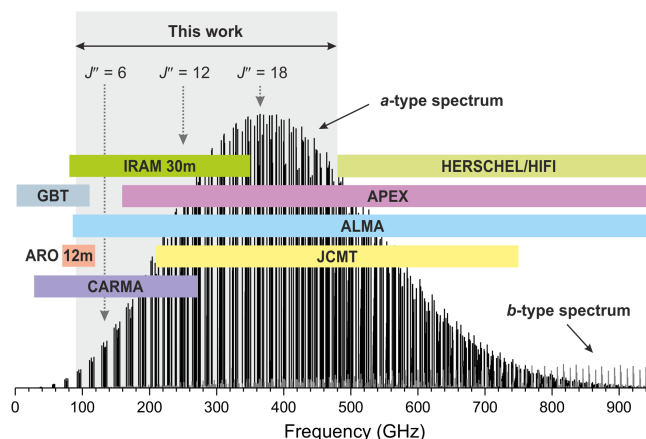


Fig. 2. Predicted rotational spectrum of methoxyamine at the temperature of 120 K and its overlap with approximate frequency coverage of several astrophysical facilities (IRAM: Institut de Radioastronomie Millimétrique; HERSCHEL/HIFI: *Herschel*-Heterodyne Instrument for the Far-Infrared; GBT: Green Bank Telescope; APEX: Atacama Pathfinder Experiment telescope; ALMA: Atacama Large Millimeter/submillimeter Array; ARO: Arizona Radio Observatory; JCMT: *James Clerk Maxwell* Telescope; CARMA: Combined Array for Research in Millimeter-wave Astronomy). The frequency region studied in this work is highlighted in gray.

3. Rotational spectra analysis

Supporting ab initio calculations were performed at the beginning of the analysis using the Gaussian09 package (Frisch et al. 2009). The Møller–Plesset second-order method (MP2) and the aug-cc-pVTZ basis set were used to geometrically optimize the structure of methoxyamine, to estimate electric dipole moment components along the principal axis, and to obtain the information on equilibrium quartic centrifugal distortion constants. Methoxyamine possesses a plane of symmetry, and its optimized geometry is illustrated in Fig. 1 (a similar geometry has been calculated by Hays & Widicus Weaver 2013). Equilibrium spectroscopic constants are given in the last column of Table 1. The calculated dipole moment components of $|\mu_a| = 0.5$ D, $|\mu_b| = 0.1$ D, and $|\mu_c| = 0.0$ D are in agreement with the fact that only a -type transitions were observed in the previous microwave work of Fong et al. (1974).

Groups of a -type R -branch transitions repeating approximately every 19 GHz were easily identified in the broadband rotational spectrum. Figure 3 shows one of these groups for $J' \leftarrow J'' = 10 \leftarrow 9$ with typical arrangement of individual K_a transitions common for a near-prolate asymmetric top ($\kappa = -0.93$ in this case). A few a -type transitions with $K_a = 1, 3, 4, 5,$ and 6 were found as doublets situated closely around the semi-rigid rotor pattern. This doublet structure originates from internal rotation of the methyl group and agrees with the relatively high barrier to internal rotation of $V_3 = 873 \pm 15$ cm⁻¹ determined by Fong et al. (1974). After we assigned the a -type transitions, we attempted to locate b -type transitions, although the value of μ_b predicted by ab initio calculations is very low. Surprisingly, many b -type R -branch and Q -branch transitions were successfully identified. While only a few a -type transitions were found to be subject to the $A-E$ splitting, almost all b -type transitions appeared as doublets, and the separation of the two lines of the doublets was less than 10 MHz. Additionally, weak forbidden x -type and c -type transitions between the E -levels (Woods 1966), which borrow intensity from allowed a -type and b -type transitions, respectively, could occasionally be observed

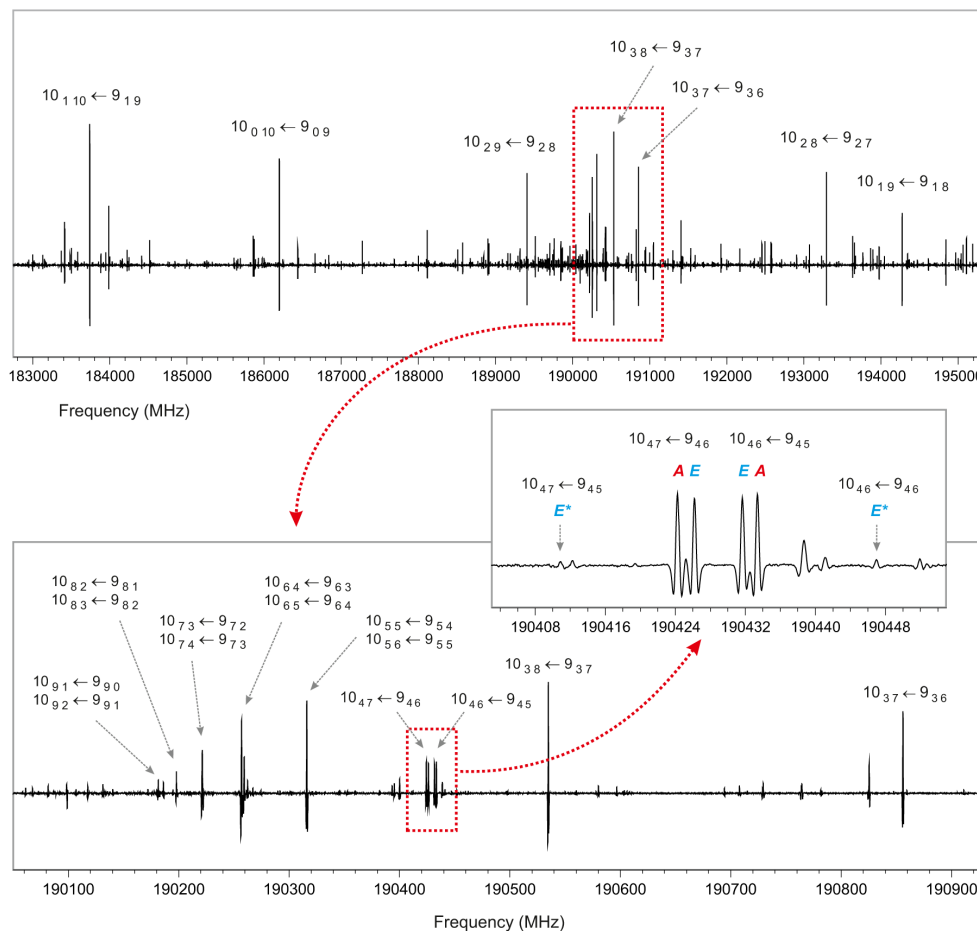


Fig. 3. Portion of the room-temperature millimeter-wave spectrum of methoxyamine showing a group of a -type R -branch transitions for $J' \leftarrow J'' = 10 \leftarrow 9$. The asymmetry splitting for the $K_a = 1$ transitions in this case reaches almost 11 GHz and decreases rapidly with increasing K_a until it is completely unresolved for $K_a \geq 5$. Small internal rotation A – E splitting can be seen for two $K_a = 4$ rotational transitions. Forbidden x -type transitions ($\Delta K_a = 0, \pm 2, \dots$, $\Delta K_c = 0, \pm 2, \dots$) that gain intensity through the so-called intensity borrowing from allowed a -type transitions between the same pairs of levels are situated outside the A lines and are labeled with an E^* .

(see the middle part of Fig. 3) in situations where the asymmetry splitting became comparable in magnitude with the internal rotation splitting (Herschbach & Swalen 1958; Plummer et al. 1987). More than 400 distinct frequency lines were finally assigned to the ground torsional state of methoxyamine. More than 100 lines correspond to A -symmetry species, more than 100 lines to E -symmetry species, and over 200 lines reveal unresolved A – E splitting. The ^{14}N nuclear quadrupole hyperfine structure could be partly resolved for transitions where the value of K_a approaches the value of J and corresponding transitions were not taken into consideration. These transitions are expected to be weak and are not interesting for a possible detection in the ISM.

Initially, A and E transitions were analyzed separately using the SPFIT/SPCAT programs (Pickett 1991). The effective rotational and centrifugal distortion constants for the A sublevels were obtained by fitting the standard Watson S -reduced Hamiltonian in I' representation (Watson 1977). In determining the E sublevel constants, Watson's semirigid Hamiltonian was extended by the linear terms $D_a J_a$ and $D_b J_b$ (Lin & Swalen 1959; Demaison et al. 2010). Finally, only D_a parameter and its centrifugal distortion corrections were determinable. The results of both fits are collected in the first two columns of Table 1. The same sets of A and E transitions were subsequently fitted using the XIAM program (Hartwig & Dreizler 1996) in order to obtain the barrier to the internal rotation V_3 of the methyl group. As

shown in Table 1, its value compares well with that from the microwave study of Fong et al. (1974). Although the effective fits for the two internal rotation sublevels as well as the XIAM fit are able to reproduce the A – E split transitions near the experimental accuracy, it has to be noted that around 50% from the observed lines were not included in these fits because of the unresolved A – E splitting. Therefore, another fit using the ERHAM program (Groner 1997), which allows proper weighting of blended transitions, was performed in this work. In this way, it was possible to encompass all the measured a -type transitions with $J'' = 3$ –24 and $K_a'' = 0$ –13 and b -type transitions with $J'' = 4$ –35 and $K_a'' = 0$ –5. This coverage of the rotational quantum numbers extends well beyond the absorption maximum at 120 K (see Fig. 2), so that the lines most likely to be detected toward the interstellar clouds are now well characterized. Table 1 presents the resulting set of 18 adjusted spectroscopic parameters, while the experimental frequencies are collected in Table 3. Among the floated parameters are rotational constants, centrifugal distortion constants up to the sixth order, internal rotation parameters ρ and β , and the first energy tunneling parameter ε_1 . Because about 50% of the assigned lines belong to the b -type transitions, which were not found in the previous work of Fong et al. (1974), the value of the A rotational constant has been significantly improved (see Table 1). The derived spectroscopic constants are in good agreement with those predicted by ab initio calculations.

Table 1. Ground-state spectroscopic constants of methoxyamine.

	SPFIT		XIAM	ERHAM	Fong et al. (1974)	Ab initio ^d
	A species ^a	E species ^a	A + E ^b	A + E ^c		
A / MHz	42 487.2256 (67) ^e	42 485.5971 (51)	42 486.1426 (34)	42 486.1402 (30)	42 488 (150)	42 457
B / MHz	10 049.6972 (13)	10 049.6652 (11)	10 051.6212 (33)	10 049.67650 (39)	10 049.59 (3)	10 137
C / MHz	8962.8910 (14)	8962.8895 (12)	8960.9454 (33)	8962.89087 (32)	8962.85 (3)	9038
D _J / kHz	9.7862 (55)	9.7854 (48)	9.7862 (25)	9.78791 (72)	...	9.72
D _{JK} / kHz	3.575 (20)	1.967 (17)	2.492 (10)	2.4821 (46)	...	2.66
D _K / kHz	471.46 (38)	443.32 (29)	452.94 (18)	452.89 (14)	...	443.97
d ₁ / kHz	-1.5834 (15)	-1.5876 (11)	-1.59121 (76)	-1.58560 (41)	...	-1.57
d ₂ / kHz	0.33027 (33)	0.33762 (29)	0.33992 (19)	0.33504 (12)	...	0.34
H _J / Hz	0.0200 (78)	0.0168 (67)	0.0178 (40)	0.02053 (69)
H _{JK} / Hz	-0.163 (35)	-0.132 (26)	-0.155 (17)	-0.1751 (35)
H _{KJ} / Hz	1.88 (88)	-17.77 (70)	-11.23 (43)	-11.001 (27)
H _K / Hz	124.4 (92)	-19.9 (73)	32.1(44)	29.4 (23)
h ₁ / Hz	0.0030 (15)	0.0091 (11)	0.00622 (74)	0.00572 (35)
h ₂ / Hz	-0.0039 (11)	-0.00786 (87)	-0.00625 (55)	-0.00571(15)
h ₃ / Hz	-0.00153 (33)	-0.00181 (26)	-0.00191 (17)	-0.001988 (34)
D _a / MHz	...	-4.074 (35)
D _a ^j / MHz	...	0.001595 (56)
D _a ^k / MHz	...	0.1711 (27)
D _a ^{kk} / MHz	...	-0.002096 (61)
ρ / Unitless	0.23864 (19)	0.23869 (15)	...	0.23
β / °	8.256 (13)	8.322 (12)	...	9.5
ε ₁ / MHz	-4.7796 (53)
V ₃ / cm ⁻¹	855.66 (52)	...	873 (15) ^f	...
σ _{fit} ^g / kHz	49	35	33	46
N ^h	119	108	227	434	4	...

Notes. ^(a) These constants are contaminated by contribution of the internal rotation. Unperturbed values that can be compared with those from the global A + E fits or from ab initio calculations can be obtained, for example, using the approximate expression $(X_A + 2X_E)/3$ (Gordy & Cook 1984), where X substitutes the rotational and centrifugal distortion constants. ^(b) Additionally derived internal rotation parameters: angles between the internal rotation axis *i* and the principal axis $\angle(i, a) = 31.522$ (42)°, $\angle(i, b) = 58.478$ (42)°, $\angle(i, c) = 90^\circ$ (fixed value), moment of inertia of the methyl top $I_\alpha = 3.2956$ (40) uÅ². ^(c) Additionally derived internal rotation parameters: torsional energy difference $\Delta E_{E-A} = 14.339$ (16) MHz, $\angle(i, a) = 31.735$ (38)°, $\angle(i, b) = 58.265$ (38)°, $\angle(i, c) = 90^\circ$ (fixed value), $I_\alpha = 3.3032$ (18) uÅ², reduced rotational constant $F = 6.5347$ (27) cm⁻¹. ^(d) Equilibrium values at the MP2/aug-cc-pVTZ level of the theory. ^(e) The numbers in parentheses are 1σ uncertainties (67% confidence level) in units of the last decimal digit. ^(f) Average value obtained from three isotopic species. ^(g) Root mean square deviation of the fit. ^(h) Number of distinct frequency-fitted lines.

4. Radioastronomical observations

Methoxyamine is a complex organic molecule (COM; carbon-based molecular species with more than six atoms, see, e.g., Herbst & van Dishoeck 2009) containing hydrogen, carbon, oxygen, and nitrogen together. COMs have mostly been detected toward hot cores of high-mass star-forming regions (Belloche et al. 2009, 2014; Tercero et al. 2013, 2015) and the inner regions of low-mass protostars, that is, of hot corinos (Cazaux et al. 2003; Jørgensen et al. 2016). Nevertheless, N-bearing compounds are typically found in the former regions, whereas hot corinos are richer in O-bearing molecules like methyl formate (CH₃OCOH). Three COMs have been identified in the ISM so far that contain H, C, O, and N: NH₂CHO, CH₃NCO, and CH₃CONH₂ (see, e.g., the CDMS database¹). Although formamide (NH₂CHO) and methyl isocyanate (CH₃NCO) have both been detected in hot corinos (Martín-Doménech et al. 2017; Ligterink et al. 2017; Coutens et al. 2016), these three species together have only been detected in the hot core of Sgr B2 at the Galactic center (Rubin et al. 1971; Halfen et al. 2015; Hollis et al. 2006; Belloche et al. 2017) and in Orion KL (Turner 1991; Motiyenko et al. 2012; Cernicharo et al. 2016), the nearest hot core at 414 ± 7 pc (Menten et al. 2007). In addition, CH₃NHCHO has recently been tentatively detected in Sgr B2

(Belloche et al. 2017). On the other hand, another possible related species of methoxyamine, methylamine CH₃NH₂, has been detected in the two high-mass star-forming regions mentioned above (Kaifu et al. 1974; Cernicharo et al. 2016). Therefore, we focused the search for CH₃ONH₂ toward these high-mass star-forming regions.

Orion KL: two sets of data were used to seek for methoxyamine in this region. On the one hand, we explored the wide frequency band (80–306 GHz) of the IRAM 30 m survey of Orion KL (Tercero et al. 2010, 2015). On the other hand, we focused the search on different positions of this complex source using the ALMA Science Verification (SV) data that cover frequencies between 213.7 and 246.6 GHz. Cernicharo et al. (2016) provided the spatial distribution of several molecular species in the source. The rather similar spatial distribution of the three more abundant species containing N, O, H, and C simultaneously is remarkable: HNCO, NH₂CHO, and CH₃NCO. Moreover, these authors provided column densities for CH₃NH₂ and CH₃CONH₂. To determine the suitable position within the source for the search for methoxyamine, we created maps of the spatial distribution of methylamine using two lines that were free of blending that arise in the ALMA SV band (see Fig. 4). Unfortunately, this was not possible for acetamide, CH₃CONH₂, because of the large uncertainty of the rest frequencies at the ALMA SV frequency range (see Halfen et al. 2011, and references therein).

¹ <https://www.astro.uni-koeln.de/cdms/molecules>

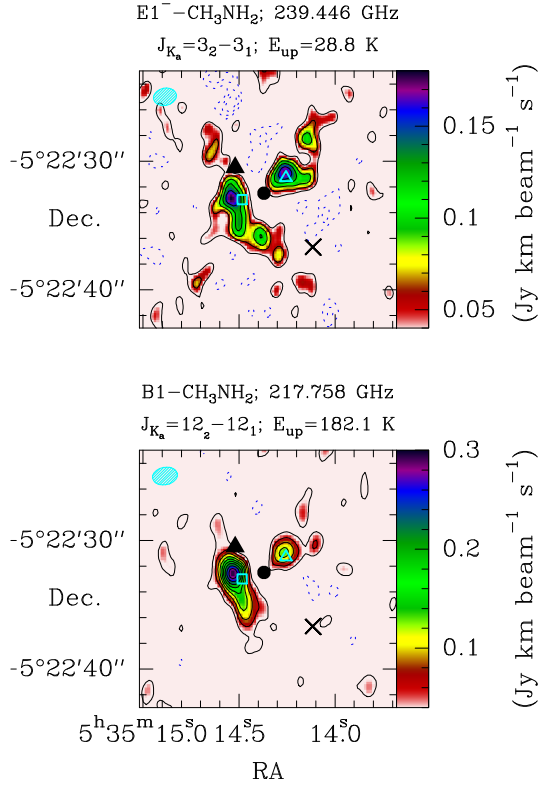


Fig. 4. Spatial distribution of CH_3NH_2 in Orion KL. The data are from ALMA SV observations. The interval of contours in black is $0.03 \text{ Jy beam}^{-1} \text{ km s}^{-1}$, and the minimum contour is $0.03 \text{ Jy beam}^{-1} \text{ km s}^{-1}$. Negative flux is represented by the blue dashed contours: the minimum contour is $-0.05 \text{ Jy beam}^{-1} \text{ km s}^{-1}$ and the interval is $-0.03 \text{ Jy beam}^{-1} \text{ km s}^{-1}$. The cyan ellipse in the top left corner of the maps represents the synthetic beam. The black triangle shows source I, the black circle shows source n, the cross represents the compact ridge, and the cyan unfilled square and triangle indicate Positions A and B (see Sect. 4).

The main emission peaks for all the species discussed above coincide with a component in the middle of the hot core clumpy structure (see, e.g., Favre et al. 2011b; Tercero et al. 2015) and the millimeter continuum source MM4 (Wu et al. 2014). These positions are described in Cernicharo et al. (2016) as positions A and B. We therefore concentrated on these two components and on the compact ridge (rich in $\text{CH}_3\text{-O}$ bearing molecules, see, e.g., Favre et al. 2011a; Brouillet et al. 2013; López et al., in prep.). We used MADEx (Cernicharo 2012) to implement the spectroscopy of CH_3ONH_2 provided in the Col. 4 of Table 1 and to derive the synthetic spectrum according to the physical parameters shown in Table 2. We did not detect methoxyamine above the detection limit of the data, hence only upper limits to the column density could be derived.

Sgr B2: we also searched for CH_3ONH_2 in public data available for Sgr B2. We did not find this species above the detection limit of the data, either in the PRIMOS survey² (Neill et al. 2012) or in the IRAM 30 m data at 3 mm provided by Belloche et al. (2013). To estimate upper limits to

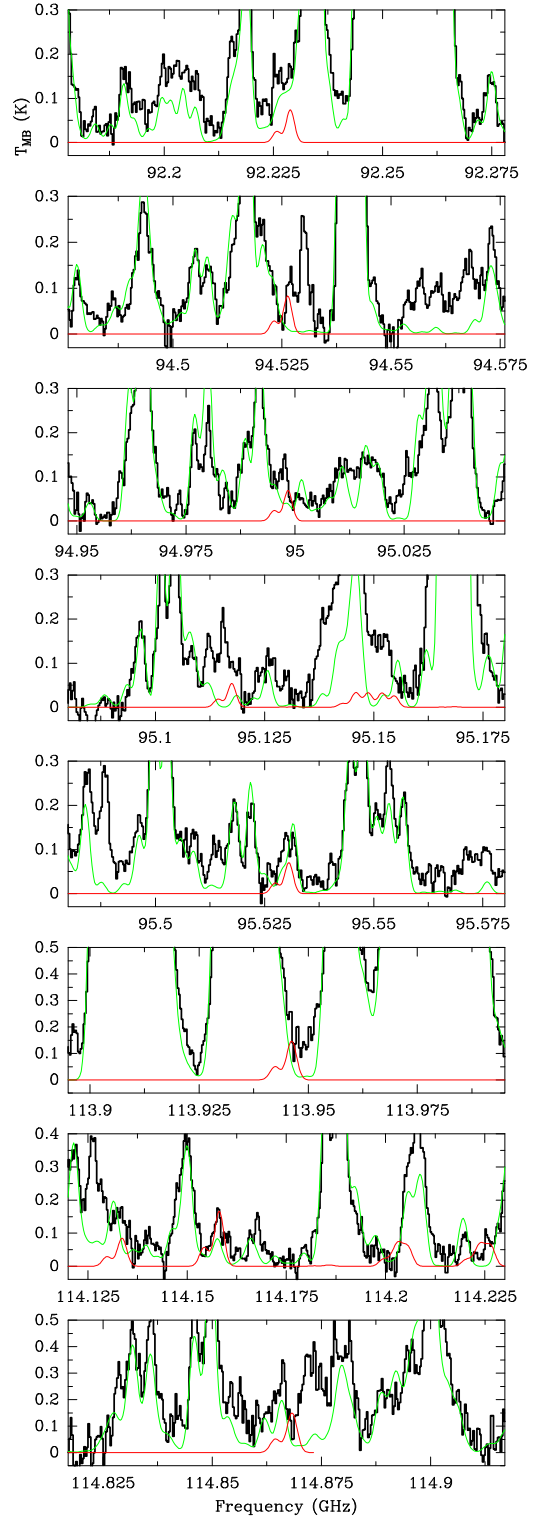


Fig. 5. Lines partially free of blending of CH_3ONH_2 in Sgr B2(N) at 3 mm. The observed data (black histogram spectrum) and total model of the source (green curve) are taken from Belloche et al. (2013). The synthetic spectrum for methoxyamine corresponding to the upper limit reported in Table 2 is given by the red line. A v_{LSR} of $+64.0 \text{ km s}^{-1}$ is assumed.

the CH_3ONH_2 column density in the region, we adopted the physical parameters derived by Belloche et al. (2013) for formamide (see Table 2). Figure 5 shows the model provided by MADEx (red line) together with the IRAM 30 m data of

² The 100 m Green Bank Telescope (GBT) PRebiotic Interstellar MOlecule Survey (PRIMOS) covers a frequency band between 7 and 50 GHz. Access to the entire PRIMOS data set, specifics on the observing strategy, and overall frequency coverage information is available at <http://www.cv.nrao.edu/~aremi/jan/PRIMOS/>

Table 2. Physical parameters of the considered cloud cores.

Source	Coordinates J2000.0	HPBW [†] (")	Frequencies ^{††} GHz	v_{LSR} (km s ⁻¹)	Δv_{FWHM} (km s ⁻¹)	d_{sou} (")	T_{rot} (K)	$N(\text{CH}_3\text{ONH}_2)$ $\times 10^{15}$ (cm ⁻²)
Orion KL (IRAM 30 m)	$\alpha = 5^{\text{h}}35^{\text{m}}14^{\text{s}}.5$ $\delta = -05^{\circ}22'30''.0$	30–8	80–307	8.0	3.0	10	150	$\leq(1.0 \pm 0.3)$
Orion KL (ALMA SV) Hot core	$\alpha = 05^{\text{h}}35^{\text{m}}14^{\text{s}}.5$ $\delta = -05^{\circ}22'32''.5$	$\sim 1.9 \times 1.4$	213.7–246.7	8.0	3.0	3.0	150	$\leq(3.0 \pm 1.0)$
Orion KL (ALMA SV) Compact ridge	$\alpha = 05^{\text{h}}35^{\text{m}}14^{\text{s}}.1$ $\delta = -05^{\circ}22'36''.9$	$\sim 1.9 \times 1.4$	213.7–246.7	7.5	2.0	3.0	100	$\leq(2.0 \pm 0.6)$
Orion KL (ALMA SV) MM4	$\alpha = 05^{\text{h}}35^{\text{m}}14^{\text{s}}.2$ $\delta = -05^{\circ}22'31''.1$	$\sim 1.9 \times 1.4$	213.7–246.7	8.0 5.0	3.0 3.0	3.0 3.0	150 150	$\leq(2.0 \pm 0.6)$ $\leq(2.0 \pm 0.6)$
Sgr B2	(IRAM 30 m) $\alpha = 17^{\text{h}}47^{\text{m}}20^{\text{s}}.0$ $\delta = -28^{\circ}22'19''.0$	30–21	80–115.5	63	7.0	2.4	180	$\leq(1000 \pm 60)$
	(GBT 100 m)			73	7.0	1.4	180	$\leq(1000 \pm 60)$
	$\alpha = 17^{\text{h}}47^{\text{m}}19^{\text{s}}.8$ $\delta = -28^{\circ}22'17''.0$	80–15	7–50	83	8.0	60	2.7	$\leq(2.0 \pm 0.6)$
B1-b (IRAM 30 m)	$\alpha = 03^{\text{h}}33^{\text{m}}20^{\text{s}}.8$ $\delta = 31^{\circ}07'34''.0$	30–21	80–115.5	6.7	0.7	60	12	$\leq(0.0020 \pm 0.0006)$
TMC-1 (IRAM 30 m)	$\alpha = 04^{\text{h}}41^{\text{m}}41^{\text{s}}.88$ $\delta = 25^{\circ}41'27''.0$	30–21	80–115.5	6.0	0.7	60	10	$\leq(0.0020 \pm 0.0006)$

Notes. ^(†) Half-power beam width (HPBW) for observations with single-dish telescopes (IRAM 30 m and GBT 100 m) and synthetic beam for the ALMA SV observations. ^(††) Range of frequencies considered in the analysis.

Sgr B2(N). Interestingly, this model is consistent with the lack of methoxyamine lines above the detection limit of the PRIMOS data.

Although we cannot claim detection, some U lines that are partially free of blending in the 30 m data agree with the modeled spectrum of this species. In addition, according to this model, we did not find missing lines. Nevertheless, this is not a strong constraint because most of the CH₃ONH₂ lines are fully blended with more abundant species in these data.

Finally, we used the data presented in [Cernicharo et al. \(2012\)](#) to derived upper limits to the methoxyamine column density in dark clouds and at different evolutionary stages (B1-b and TMC-1 clouds; see Table 2).

5. Discussion

To compare the results for the search for methoxyamine to the chemical model predictions provided by [Garrod et al. \(2008\)](#), we derived upper limits to the molecular abundance of this species in the hot core of Orion KL and Sgr B2(N).

[Tercero et al. \(2010\)](#) obtained a source-averaged $N(\text{H}_2)$ of 4.2×10^{23} cm⁻² for the hot core of Orion KL by means of the C¹⁸O column density, assuming that the CO/H₂ abundance ratio is roughly constant (2×10^{-4} in warm regions) and adopting a source diameter of 10'' for the hot core. To obtain a value for the molecular abundance, we also have to assume that the H₂ column density spatially coincides with the emission from the species considered. We derived an upper limit to the CH₃ONH₂ abundance of 2×10^{-9} using the upper limit for the column density obtained for Orion KL with the IRAM 30 m data. A large uncertainty should be associated with this value (at least a factor of 2) because of the mentioned assumptions.

On the other hand, [Belloche et al. \(2008\)](#) derived an $N(\text{H}_2)$ of 1.3×10^{25} cm⁻² in the inner region (2'') of Sgr B2(N) using

the continuum emission detected with the Plateau de Bure Interferometer (PdBI) and assuming that this continuum emission at 3.7 mm is dominated by thermal dust emission (optically thin and a dust temperature of 100 K). Further assumptions related to the dust mass opacity and the dust emissivity exponent have to be made to obtain this $N(\text{H}_2)$ value (see [Belloche et al. 2008](#), for details). We derive an upper limit to the CH₃ONH₂ abundance of $(7-8) \times 10^{-8}$ using the upper limit for the column density obtained for the 63 km s⁻¹ component of Sgr B2(N). Once again, an uncertainty of at least a factor of 2 is associated with this value ([Belloche et al. 2008](#)).

Like [Garrod et al. \(2008\)](#), we note a reasonable match in the comparison of the derived upper limit abundances (and the assumed rotational temperatures) and the results of the ‘‘reduced ice composition’’ chemical model provided by these authors. In this model, the initial ice composition (standard) was adjusted to agree with infrared observations of protostellar envelopes, reducing the amount of the ices available for primary-radical production (see [Garrod et al. 2008](#), for details). Abundances of methoxyamine in the fast (5×10^4 yr) and slow (1×10^6 yr) warm-up timescales are 3.7×10^{-9} and 6.4×10^{-8} , respectively (the rotational temperature derived is around 120 K in both models). These timescales are identified with high- and low-mass star formation, respectively ([Garrod et al. 2008](#)). It is worth noting that [Aikawa et al. \(2008\)](#) proposed a different relation between mass and warm-up timescale. They suggested that the warm-up timescale is dependent on the ratio of the size of the warm region to the infall speed, rather than on the overall speed of star formation. The abundances predicted by the model are on the same order (within the uncertainties) as the upper limits derived observationally. However, because we study two high-mass star-forming regions, these differences may indicate different initial ice compositions and/or evolutionary stages.

To check these results and to avoid the large uncertainties introduced by the estimation of the CH_3ONH_2 abundances, we also compared the observed and predicted $\text{NH}_2\text{CHO}/\text{CH}_3\text{ONH}_2$ abundance ratios. The NH_2CHO column density has been derived by Motiyenko et al. (2012) and Belloche et al. (2013) for Orion KL and Sgr B2, respectively, using similar physical parameters and the same observational data (IRAM 30 m data) as those used in this work to derive the CH_3ONH_2 column density. The derived lower limit ratios are ≥ 0.6 and ≥ 1.35 for Orion KL and the 63 km s^{-1} component of Sgr B2. The predicted results provided by the “reduced ice composition” chemical model of Garrod et al. (2008) are 27, 12, and 2 for the fast, medium, and slow warm-up timescales. The predictions of all three models are consistent with the derived lower limit ratios. Hence, by means of these ratios and according to this model, we cannot constraint the relation between mass and warm-up timescale.

6. Conclusion

The rotational spectrum of methoxyamine has been recorded from 75 to 480 GHz and over 400 lines were newly assigned for the most stable conformer. Methoxyamine has not been identified above the detection limit of various sets of data of the well-known high-mass star-forming regions Orion KL and Sgr B2. Nevertheless, the upper limits to the methoxyamine abundance in these regions agree with the CH_3ONH_2 abundances derived in chemical models. This suggests a possible positive detection of methoxyamine in the near future using high-sensitivity data of hot cores and hot corinos and the accurate spectroscopic data of this work.

Acknowledgements. This paper makes use of the following ALMA data: ADS/JAO.ALMA#2011.0.00009.SV. ALMA is a partnership of ESO (representing its member states), NSF (USA), and NINS (Japan) with NRC (Canada), NSC, and ASIAA (Taiwan), and KASI (Republic of Korea), in cooperation with the Republic of Chile. The Joint ALMA Observatory is operated by ESO, AUI/NRAO, and NAOJ. This work was also based on observations carried out with the IRAM 30-m telescope. IRAM is supported by INSU/CNRS (France), MPG (Germany), and IGN (Spain). The research leading to these results has received funding from the European Research Council under the European Union’s Seventh Framework Programme (FP/2007–2013)/ERC-2013-SyG, Grant Agreement No. 610256 NANOCOSMOS, Ministerio de Ciencia e Innovación (Grants CTQ2013-40717-P, AYA2012-32032, and Consolider-Ingenio 2010 CSD2009-00038 program “ASTROMOL”) and Junta de Castilla y León (Grants VA070A08 and VA175U13). J.-C.G. and J.C. thank the ANR-13-BS05-0008 IMOLABS. J.-C.G. thanks the Program PCMI (INSU-CNRS) and the Centre National d’Études Spatiales (CNES) for funding support. E.R.A. thanks the Ministerio de Ciencia e Innovación for FPI grant (BES-2014-067776).

References

- Aikawa, Y., Wakelam, V., Garrod, R. T., & Herbst, E. 2008, *ApJ*, **674**, 984
 Altwegg, K., Balsiger, H., Bar-Nun, A., et al. 2016, *Sci. Adv.*, **2**
 Belloche, A., Menten, K. M., Comito, C., et al. 2008, *A&A*, **482**, 179
 Belloche, A., Garrod, R. T., Müller, H. S. P., et al. 2009, *A&A*, **499**, 215
 Belloche, A., Müller, H. S. P., Menten, K. M., Schilke, P., & Comito, C. 2013, *A&A*, **559**, A47
 Belloche, A., Garrod, R. T., Müller, H. S. P., & Menten, K. M. 2014, *Science*, **345**, 1584
 Belloche, A., Meshcheryakov, A. A., Garrod, R. T., et al. 2017, *A&A*, **601**, A49
 Bernstein, M. P., Dworkin, J. P., Sandford, S. A., Cooper, G. W., & Allamandola, L. J. 2002, *Nature*, **416**, 401
 Bissot, T. C., Parry, R. W., & Campbell, D. H. 1957, *J. Am. Chem. Soc.*, **79**, 796
 Brouillet, N., Despois, D., Baudry, A., et al. 2013, *A&A*, **550**, A46
 Caro, G. M., Meierhenrich, U., Schutte, W., et al. 2002, *Nature*, **416**, 403
 Cazaux, S., Tielens, A. G. G. M., Ceccarelli, C., et al. 2003, *ApJ*, **593**, L51
 Cernicharo, J. 2012, in *ECLA-2011: Proc. of the European Conf. on Laboratory Astrophysics, Laboratory Astrophysics and Astrochemistry in the Herschel/ALMA Era*, **58**, 251
 Cernicharo, J., Marcelino, N., Roueff, E., et al. 2012, *ApJ*, **759**, L43
 Cernicharo, J., Kisiel, Z., Tercero, B., et al. 2016, *A&A*, **587**, L4
 Coutens, A., Jørgensen, J. K., van der Wiel, M. H. D., et al. 2016, *A&A*, **590**, L6
 Cunningham, M. R., Jones, P. A., Godfrey, P. D., et al. 2007, *MNRAS*, **376**, 1201
 Daly, A., Kolesníková, L., Mata, S., & Alonso, J. 2014, *J. Mol. Spectr.*, **306**, 11
 Demaison, J., Margulès, L., Kleiner, I., & Császár, A. 2010, *J. Mol. Spectr.*, **259**, 70
 Eilsa, J. E., Glavin, D. P., & Dworkin, J. P. 2009, *Meteor. Planet. Sci.*, **44**, 1323
 Favre, C., Despois, D., Brouillet, N., et al. 2011a, *A&A*, **532**, A32
 Favre, C., Wootten, H. A., Remijan, A. J., et al. 2011b, *ApJ*, **739**, L12
 Fong, M. Y., Johnson, L. J., & Harmony, M. D. 1974, *J. Mol. Spectr.*, **53**, 45
 Foukris, N., Takagi, K., & Morimoto, M. 1974, *ApJ*, **191**, L139
 Frisch, M. J., Trucks, G. W., Schlegel, H. B., et al. 2009, Gaussian 09 Revision E.01 (Wallingford CT: Gaussian Inc.)
 Garrod, R. T., Weaver, S. L. W., & Herbst, E. 2008, *ApJ*, **682**, 283
 Gordy, W., & Cook, R. L. 1984, *Microwave molecular spectra* (New York: Wiley Interscience)
 Groner, P. 1997, *J. Chem. Phys.*, **107**, 4483
 Halfen, D. T., Ilyushin, V., & Ziurys, L. M. 2011, *ApJ*, **743**, 60
 Halfen, D. T., Ilyushin, V. V., & Ziurys, L. M. 2015, *ApJ*, **812**, L5
 Hartwig, H., & Dreizler, H. 1996, *Z. Naturforsch. A*, **51**, 923
 Hays, B. M., & Widicus Weaver, S. L. 2013, *J. Phys. Chem. A*, **117**, 7142
 Herbst, E., & van Dishoeck, E. F. 2009, *Ann. Rev. Astron. Astr.*, **47**, 427
 Herschbach, D. R., & Swalen, J. D. 1958, *J. Chem. Phys.*, **29**, 761
 Hollis, J. M., Lovas, F. J., Remijan, A. J., et al. 2006, *ApJ*, **643**, L25
 Jones, P. A., Cunningham, M. R., Godfrey, P. D., & Cragg, D. M. 2007, *MNRAS*, **374**, 579
 Jørgensen, J. K., van der Wiel, M. H. D., Coutens, A., et al. 2016, *A&A*, **595**, A117
 Kaifu, N., Morimoto, M., Nagane, K., et al. 1974, *ApJ*, **191**, L135
 Kim, Y. S., & Kaiser, R. I. 2011, *ApJ*, **729**, 68
 Kuan, Y.-J., Charnley, S. B., Huang, H.-C., Tseng, W.-L., & Kisiel, Z. 2003, *ApJ*, **593**, 848
 Ligterink, N. F. W., Coutens, A., Kofman, V., et al. 2017, *MNRAS*, **469**, 2219
 Lin, C. C., & Swalen, J. D. 1959, *Rev. Mod. Phys.*, **31**, 841
 Martín-Doménech, R., Rivilla, V. M., Jiménez-Serra, I., et al. 2017, *MNRAS*, **469**, 2230
 McGuire, B. A., Carroll, P. B., Dollhopf, N. M., et al. 2015, *ApJ*, **812**, 76
 Menten, K. M., Reid, M. J., Forbrich, J., & Brunthaler, A. 2007, *A&A*, **474**, 515
 Motiyenko, R. A., Tercero, B., Cernicharo, J., & Margulès, L. 2012, *A&A*, **548**, A71
 Neill, J. L., Muckle, M. T., Zaleski, D. P., et al. 2012, *ApJ*, **755**, 153
 Pickett, H. M. 1991, *J. Mol. Spectr.*, **148**, 371
 Plummer, G. M., Herbst, E., & De Lucia, F. C. 1987, *ApJ*, **318**, 873
 Pulliam, R. L., McGuire, B. A., & Remijan, A. J. 2012, *ApJ*, **751**, 1
 Remijan, A. J., Snyder, L. E., McGuire, B. A., et al. 2014, *ApJ*, **783**, 77
 Rubin, R., G. W. Swenson, J., Benson, R., Tigelaar, H., & Flygare, W. 1971, *ApJ*, **169**, L39
 Snyder, L. E., Lovas, F. J., Hollis, J. M., et al. 2005, *ApJ*, **619**, 914
 Tercero, B., Cernicharo, J., Pardo, J. R., & Goicoechea, J. R. 2010, *A&A*, **517**, A96
 Tercero, B., Kleiner, I., Cernicharo, J., et al. 2013, *ApJ*, **770**, L13
 Tercero, B., Cernicharo, J., López, A., et al. 2015, *A&A*, **582**, L1
 Turner, B. E. 1991, *ApJS*, **76**, 617
 Turner, B., Liszt, H., Kaifu, N., & Kisliakov, A. 1975, *ApJ*, **201**, L149
 Watson, J. K. G. 1977, in *Vibrational Spectra and Structure*, ed. J. R. Durig (Amsterdam: Elsevier), **6**, 1
 Woods, R. 1966, *J. Mol. Spectr.*, **21**, 4
 Wu, Y., Liu, T., & Qin, S.-L. 2014, *ApJ*, **791**, 123
 Zheng, W., & Kaiser, R. I. 2010, *J. Phys. Chem. A*, **114**, 5251